Integrated Geological and Geophysical Interpretation for the Koodaideri Detrital Iron Deposits, Fortescue Valley, Western Australia

James Reid*
Mira Geoscience
45 Ventnor Ave, West Perth, WA
jamesr@mirageoscience.com

James Farrell
Mira Geoscience
45 Ventnor Ave, West Perth, WA
jamesf@mirageoscience.com

Glenn Pears
Mira Geoscience
39 Sherwood Rd, Toowong, QLD
glennp@mirageoscience.com

Andrew Jaunzems
Rio Tinto Exploration
37 Belmont Ave, Belmont, WA
Andrew.Jaunzems@riotinto.com

Mike Enright
Rio Tinto Exploration
37 Belmont Ave, Belmont, WA
Mike.Enright@riotinto.com

Mike Haederle
Rio Tinto Exploration
37 Belmont Ave, Belmont, WA
Mike.Haederle@riotinto.com

**presenting author asterisked*

SUMMARY

This paper presents a review of integrated interpretation of geophysical surveys with geological data for interpretation and exploration targeting for detrital iron deposits at the Koodaideri Project, Western Australia. Significant previous exploration has been conducted in the area and this has identified a number of detrital iron deposits. The aim of this project has been to integrate all available geoscientific data in order to assess remaining prospectivity of the area and provide a framework for future exploration and evaluation projects.

Previous exploration at Koodaideri has used a variety of techniques including drilling, downhole geophysical logs, sparse refraction seismic, airborne and ground gravity, airborne magnetics and time-domain airborne electromagnetics. Spatial coverage of the individual exploration datasets is irregular, and the first stage of this project has focussed on an area of approximately 42 km × 12 km within which there is reasonably good coverage of all data types. The relatively high data density has allowed the relationships between the various data types to be assessed and effective exploration parameters to be defined.

The larger detrital iron deposits at Koodaideri occur within palaeochannels or depressions within the basement, which is mainly comprised of units of the Wittenoom Formation. The detrital iron deposits are considered to have been sourced from erosion of bedded iron deposits of the Brockman Iron Formation which outcrops on the high ground both upstream and immediately to the southwest of the area of interest. The known deposits generally occur beneath cover of variable thickness of up to 50 m. The detrital deposits themselves may have thicknesses in excess of 100 m in major palaeochannels and sinkholes. The detrital deposits have a higher density than other cover units due to their high iron content (>50% Fe). However, gravity alone is not an effective exploration technique because the gravity signature is complicated by significant variability in the depth to higher density Wittenoom Formation bedrock. A more recent development is use of a modified seismic refraction method (Sparse Refraction Seismic) to constrain the basement topography, and then to model and remove the basement response from the observed gravity data to identify areas of anomalous excess mass. This approach has allowed cost-effective semi-regional exploration and has been successful in identifying all known major detrital iron deposits.

This study extended the excess mass approach by constructing revised basement models from the sparse refraction seismic and drilling and from interpretation of the SkyTEM airborne electromagnetic and drilling. The results show that the basement interface can be interpreted from either the seismic or airborne electromagnetic datasets, although the airborne electromagnetic interpretation is complicated by highly saline groundwater in the northeastern quadrant of the area and by conductive shale units within the Wittenoom Formation bedrock. Almost all of the known detrital and channel iron deposits are spatially associated with an overlying pisolite unit, which can be identified from the magnetic data via its characteristic magnetic texture.

These studies have shown that the derived excess mass is spatially associated with the known detrital and channel iron mineralisation. Significantly, almost all of the known deposits were also successfully identified from the simple geological model, in the absence of drill hole constraints. A number of untested areas of possible mineralisation have been identified, as well as potential extensions or alternate trends to known mineralisation.

The modelling scenarios tested confirmed that the minimum elements for exploration targeting at Koodaideri are a geological model incorporating basement topography, interpreted magnetic domains and geologically constrained inversion of the gravity data.

Key words: refraction seismic, gravity, magnetics, iron ore exploration, geological modelling.

INTRODUCTION

The southern margins of the Fortescue Valley abutting the rangefront some 50 km either side of the Koodaideri bedded iron deposits host detrital iron deposits (DID) that are concentrated in topographic depressions in the palaeosurface. Basement outcrops as a few isolated outliers in a vast featureless plain of recent alluvials. The area of interest for this study covers an area of 42 km × 12 km, as shown in Figure 1.

The geology at Koodaideri includes basement rocks of the late Archean to early Proterozoic Hamersley Group which are buried under a Cenozoic detrital sequence. The stratigraphy of the detritals includes a lower sequence of hematitic detritals, cemented detritals , clays and a pisolite cap. Overlying the lower detritals is an upper sequence of clays, and siliceous "immature" detritals. The target mineralisation for the area is the variably cemented hematitic detritals, which occurs in the lower detrital sequence.

Previous exploration at Koodaideri has used a variety of techniques including drilling, downhole geophysical logs, sparse refraction seismic, airborne and ground gravity, airborne magnetics and time-domain airborne electromagnetics. Survey coverage within the Area of Interest is shown in Figure 2.

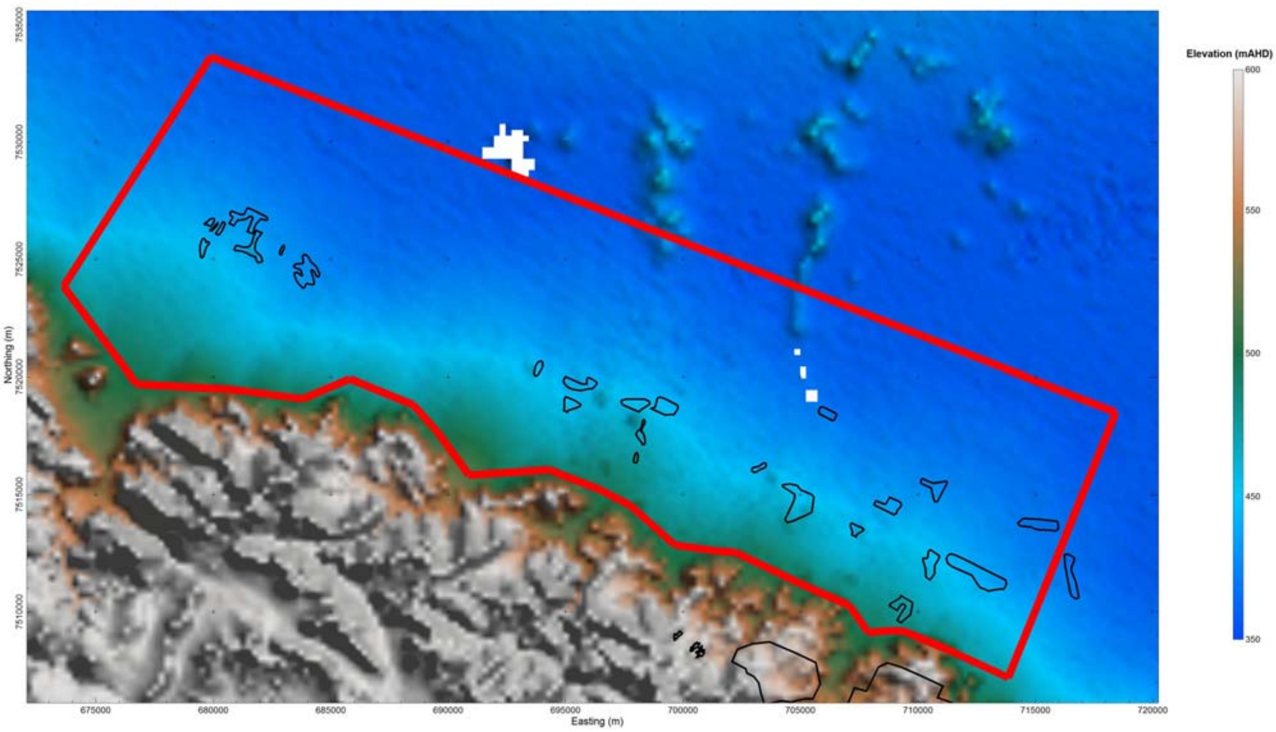

Figure 1 Area of interest for the Koodaideri Detritals study (red polygon). The black polygons within the Area of Interest show known DIDs. The underlying image is the digital elevation model. Coordinates are MGA51.

EXPLORATION METHODS

The main datasets on which the interpretation was based are summarised briefly below:

Drilling

There are approximately 1400 reverse circulation drillholes within the area of interest, drilled between 1974 and 2015. A small number of diamond drill holes have also been completed.

Ground gravity

Surface gravity coverage is shown in Figure 2. The typical station spacing is 100 m along lines parallel to the rangefront with a spacing of 400 m between lines. Gravity processing has involved terrain correction, calculation of the first vertical derivative (1VD) and high-pass filtering. Because 1VD filtering suppresses the regional response, and emphasises near-surface features, this component (G_{zz}) has been used for modelling.

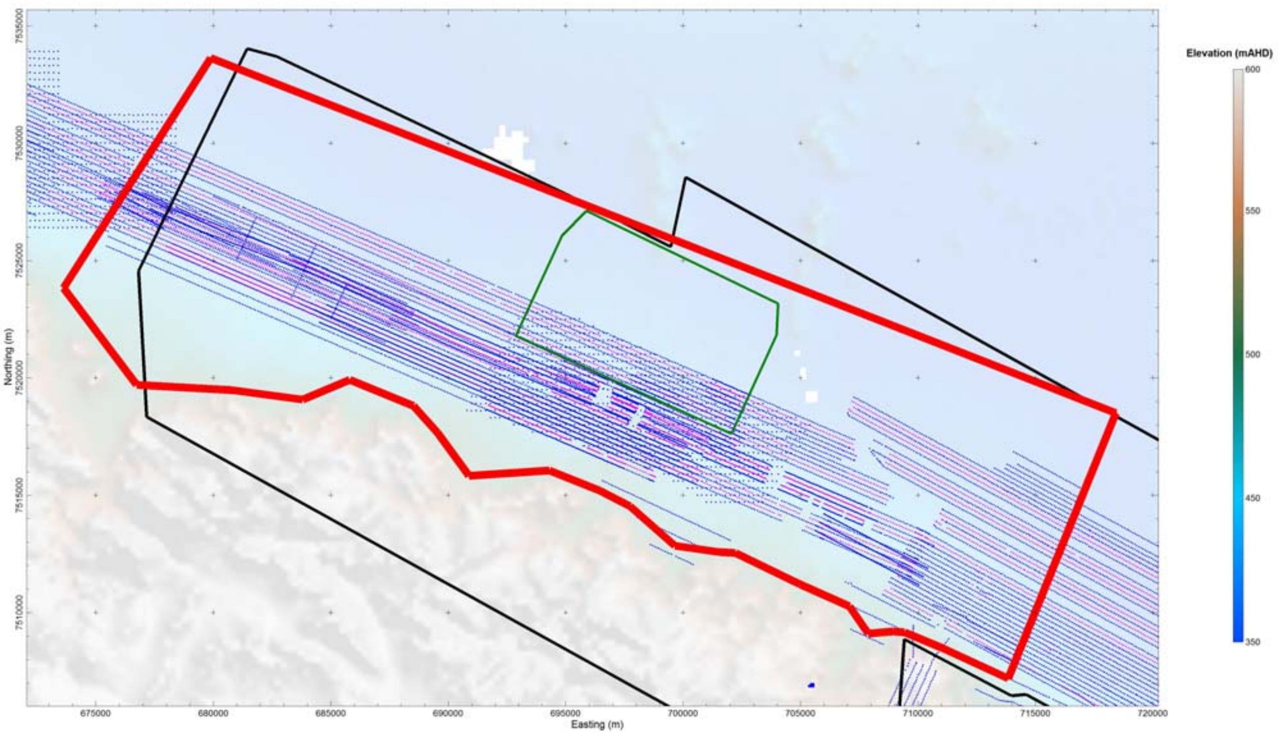

Figure 2 Geophysical data coverage within the Area of Interest at Koodaideri (red polygon). Surveys shown are: ground gravity (dark blue); sparse refraction seismic (pink); HeliFALCON airborne gravity gradiometry (green polygon); SkyTEM AEM (black polygon).

Sparse refraction seismic

Seismic methods are appropriate for mapping of the palaeotopographic surface given the large velocity contrast between the cover (1400 m/s) and basement (7000 m/s).

Sparse refraction seismic (SRS) is a greatly simplified version of traditional refraction seismic. For each shotpoint, SRS seismic data was recorded at three receivers – one 400 m ahead of the shot and two located 400 m either side of the shot in a direction orthogonal to the shot line. Shots were located every 100 m along line. First breaks were picked from the data and were used to calculate an approximate depth to the first refractor based on assumed cover and basement velocities. These assumed velocities were calculated at the start of each day's acquisition via a more conventional refraction shot, using first break data recorded at multiple offsets from the shot assuming a two or three-layered model. Calculated depths were plotted at the shot-receiver midpoints, resulting in three parallel lines of data 200 m apart, with an along-line station spacing of 100 m.

SRS acquisition was very efficient, with ~7 line km of data acquisition per day at a shot spacing of 100 m, and with data recorded simultaneously on the two parallel receiver lines. The shot-receiver offsets employed were suitable for determining depth to basement for cover thicknesses of up to 170 m, based on assumed cover and basement velocities of 1400 m/s and 7000 m/s respectively. Gravity data was collected concurrently with the SRS data, as this was found to be logistically efficient.

There were two main complications encountered in interpretation of the SRS data. More consolidated units within the cover (e.g. cemented detrital or calcrete units) have a relatively high seismic velocity and may result in erroneously-shallow depth to basement estimates. Large sinkholes within the dolomites of the Paraburdoo Member of the Wittenoom Formation may have diameters of several hundred metres and depth to basement in excess of 150 m. SRS data indicates increasing cover thickness at the edges of sinkholes, but does not yield reliable estimates of the maximum depth to bedrock determined via drilling. This may be because either the SRS-determined depth to bedrock represents an average value between the shot and receiver, or because the refracted wave travels around the edges of the sinkhole, outside the shot-receiver plane.

Airborne gravity gradiometry

Airborne gravity gradiometry (AGG) data was acquired using the HeliFalcon system over a 10 km × 5 km block located roughly in the centre of the Area of Interest (Figure 2). The main survey lines were flown parallel to the rangefront (SE-NW) at a spacing of 100 m, and SW-NE tie lines were flown at 1 km spacing. Nominal survey terrain clearance was 40 m.

Airborne Magnetics

Several generations of airborne magnetic data have been flown at Koodaideri, often as part of Hoistem time-domain airborne electromagnetic (AEM) surveys. Line spacing is typically 200 m with a sensor height of 45 m.

Airborne Electromagnetics

A number of time-domain airborne electromagnetic surveys have been flown at Koodaideri, using GEOTEM, Hoistem and, most recently, SkyTEM[508]. The SkyTEM dataset was used in this study as it had had the most complete data coverage. Survey lines were flown parallel to the rangefront (SE-NW) at a spacing of 500 m. Nominal terrain clearance was 40 m. The SkyTEM data were inverted for a 30-layer smooth model using the inversion program HyTEM (Christensen and Tølbøll, 2009).

METHOD AND RESULTS

The stratigraphy of the Koodaideri detritals includes a lower sequence of detrital iron-rich sediments, cemented detritals, clays and a pisolite cap. Overlying the lower detritals is an upper sequence of clays, and siliceous "immature" detritals. The lower detrital sequence is ascribed to the Cenozoic Detritals 2 (CzD2) and the upper detrital sequence is ascribed to the Cenozoic Detritals 3 (CzD3) of Kneeshaw and Morris (2014).

Figure 3 shows an image of the 1VD of the high-pass filtered and reduced to pole magnetics magnetic data, with mineralised drillholes superimposed. A prominent zone of mottled magnetic texture has been interpreted as the pisolite layer between the upper and lower detritals. There is a strong spatial correlation between the interpreted pisolite and high-grade iron mineralisation. Only one known DID occurs outside the interpreted extent of the pisolite – this is possibly where the pisolite layer is thinner or has been eroded subsequent to deposition.

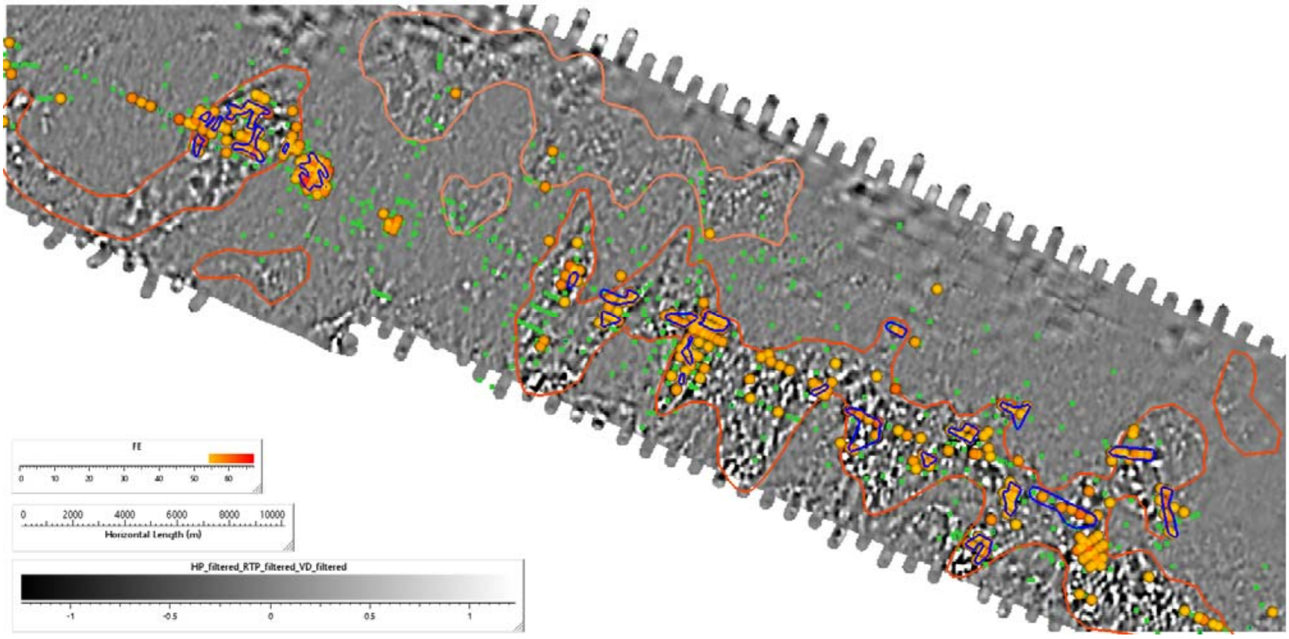

Figure 3 1VD of the high-pass filtered and reduced to pole magnetics, showing drill hole collars (green points), samples >54% Fe (orange points) and existing deposits (blue polygons). Red and orange polygons enclose zones of mottled magnetic texture interpreted as pisolites.

Excess mass from depth to basement from SRS and drilling

Raw gravity data from Koodaideri shows poor correlation with known DIDs because the gravity signature is strongly influenced by the highly-irregular cover-basement interface. Accordingly, the effect of cover thickness variations has been modelled in 3D and removed from the gravity data in order to highlight density anomalies ('excess mass') potentially associated with DID mineralisation. This approach identifies density anomalies within both the cover and basement: zones of excess mass corresponding to local basement depressions are considered more likely to be associated with DID mineralisation.

Figure 4 shows an image of the interpreted depth to basement derived from drilling and SRS data. This response of this basement model was calculated assuming an average cover density of 2.2 g/cm^3 and a basement density of 3.0 g/cm^3. These density values were derived from existing petrophysical data, density measurements on drillhole samples and numerical modelling experiments. The gravity response of the basement model was subtracted from the observed gravity data to produce a residual response due to the excess mass. Geologically-constrained inversion using the depth to basement model then allowed this residual response to be reconciled in terms of 3D density variations within the cover. Figure 5 shows an excess mass image produced using a density threshold of 2.47 g/ cm^3 and filtered to remove small-scale features containing less than 200 adjacent voxels. The excess mass image successfully identifies all known major DIDs, as indicated by the high-grade Fe in the drill hole intersections. There are also a number of excess mass anomalies which have not yet been drill tested, and which represent potential targets for future exploration.

A number of more complicated gravity models were also attempted, which incorporated density variations between the units in the cover, including the upper and lower detritals, clay layers and pisolite. Petrophysical control on the densities of these cover units was obtained from gamma density logs, which were quality controlled to exclude low-reliability data. However, excess mass derived from these more complicated models was found to be essentially identical to that derived from the simplified two-layer model.

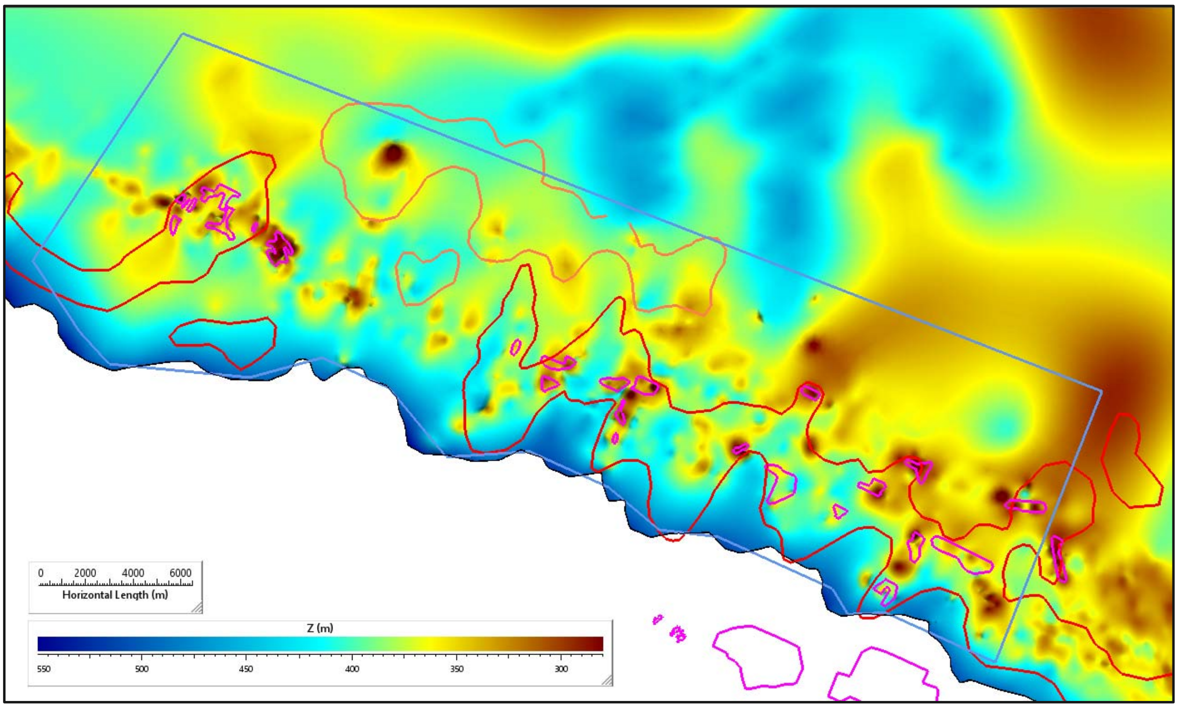

Figure 4 Basement model derived from Sparse Refraction Seismic and drilling data, coloured by elevation. Known deposits are shown as pink polygons. Warmer colours denote basement depressions. The blue polygon shows the Area of Interest. Red and orange polygons denote the interpreted pisolites.

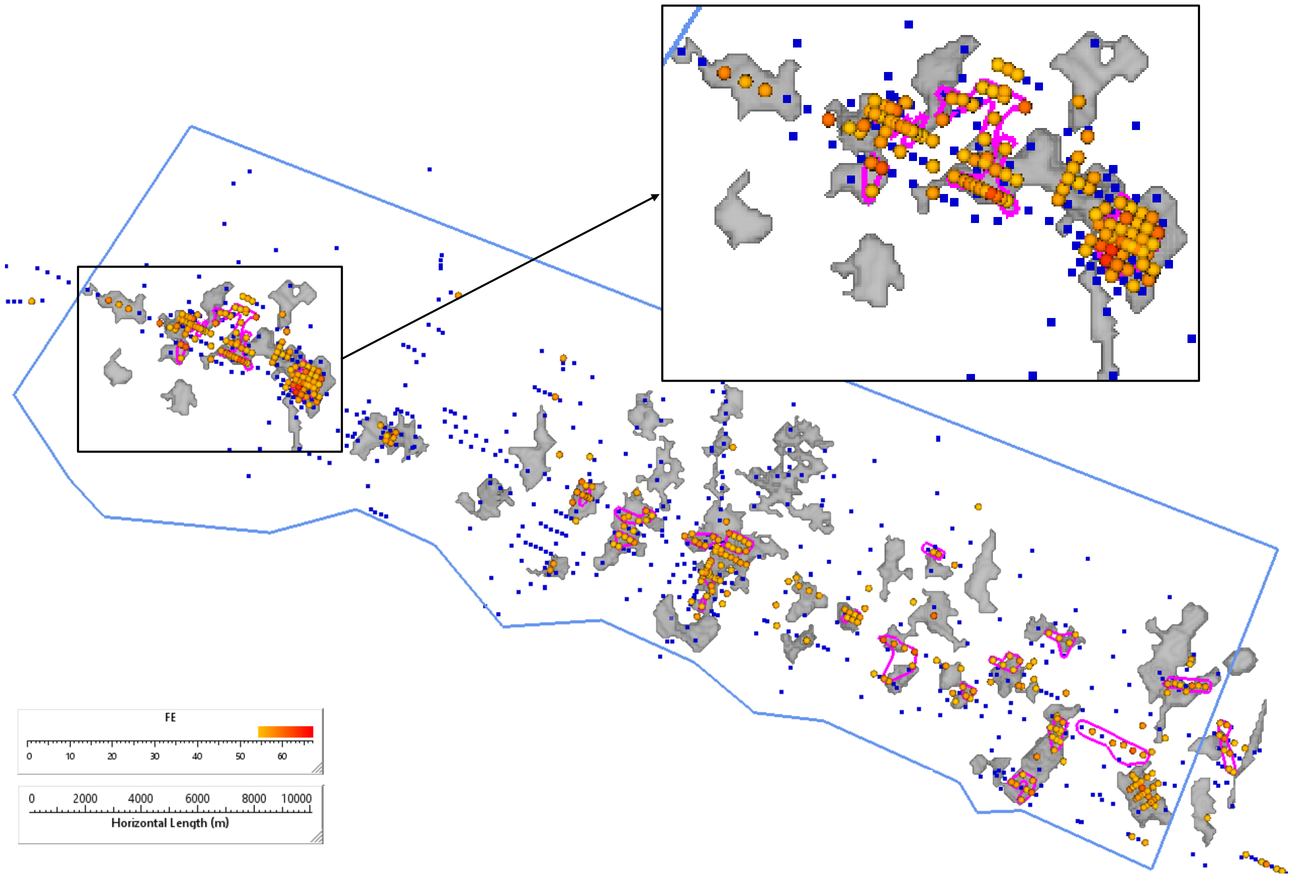

Figure 5 Excess mass from the sparse refraction seismic cover thickness model, showing drill holes and samples with >54% Fe.

Excess mass from depth to basement from SkyTEM AEM

There are a number of known limitations of the excess mass image shown in Figure 5. Where the basement is reasonably shallow, the depth to bedrock determined using the SRS method is an average value between the shot and receiver. The true depth to basement within large sinkholes within the Wittenoom Formation may be underestimated as a result of either lateral averaging or because the refracted wave may travel around the edge of the sinkhole rather than via its deepest point. The method may also give erroneously-shallow depth to bedrock estimates where high-velocity units (e.g., cemented detritals) are present within the cover. Because of the known limitations of the depth to basement model, a second model was produced based on interpretation of depth to basement from the SkyTEM AEM data. Although the units within the cover are generally moderately conductive, the conductivity contrast with the unweathered basement is highly variable. Basement units such as the gently SSW-dipping Mt McRae Shale and the Bee Gorge Member of the Wittenoom Formation are electrically-conductive, whereas others such as the Dales Gorge Member of the Brockman Iron Formation, and the Paraburdoo Member of the Wittenoom Formation are generally resistive (Figure 6, Figure 7). The section in Figure 7 is oriented perpendicular to the flight line direction and has low along-line resolution due to the 500 m flight line spacing. The break in the Bee Gorge Member in the centre of Figure 7 is interpreted to be associated with the Poonda Fault, which trends NW-SE across the area of interest.

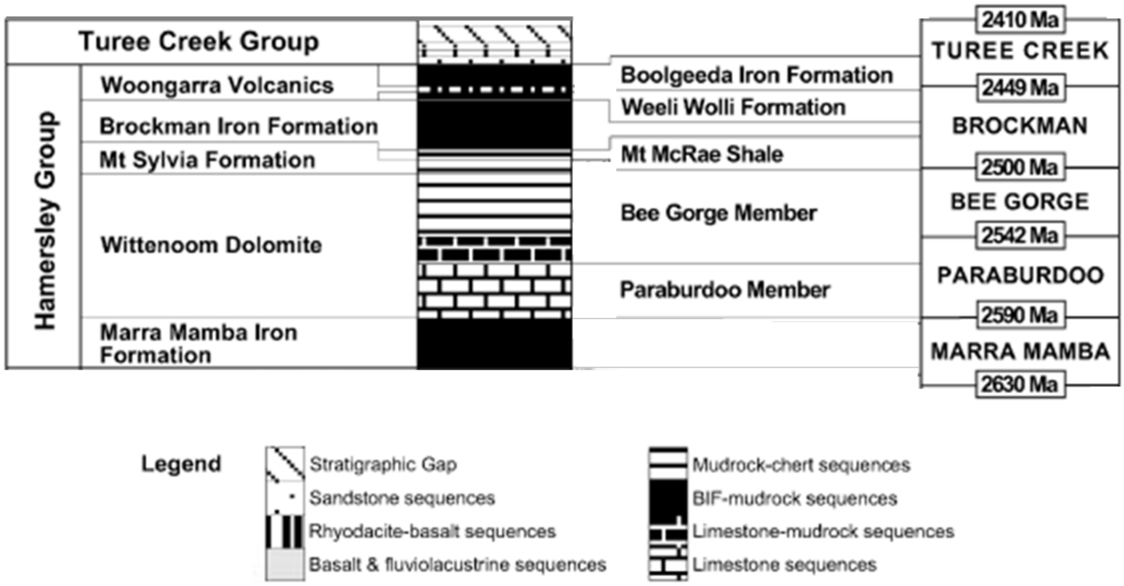

Figure 6 Stratigraphy of the Koodaideri area, modified from Figure 2 of Krapež et al. (2003). The Wittenoom Dolomite is now commonly referred to as the Wittenoom Formation.

Interpretation of the AEM data for cover thickness was complicated by the presence of highly saline groundwater in the northeast of the area of interest. The water table conductor can often be recognised because it is very flat-lying. Cover thickness was manually interpreted from each AEM conductivity-depth section independent of drill hole information, and a top basement surface was subsequently by combining the AEM interpretation and drilling, with precedence given to the drilled basement depth (Figure 8). The excess mass derived from the AEM (Figure 9) and drilling-derived basement identified the same major features as that from the SRS and drilling data, although there were some differences.

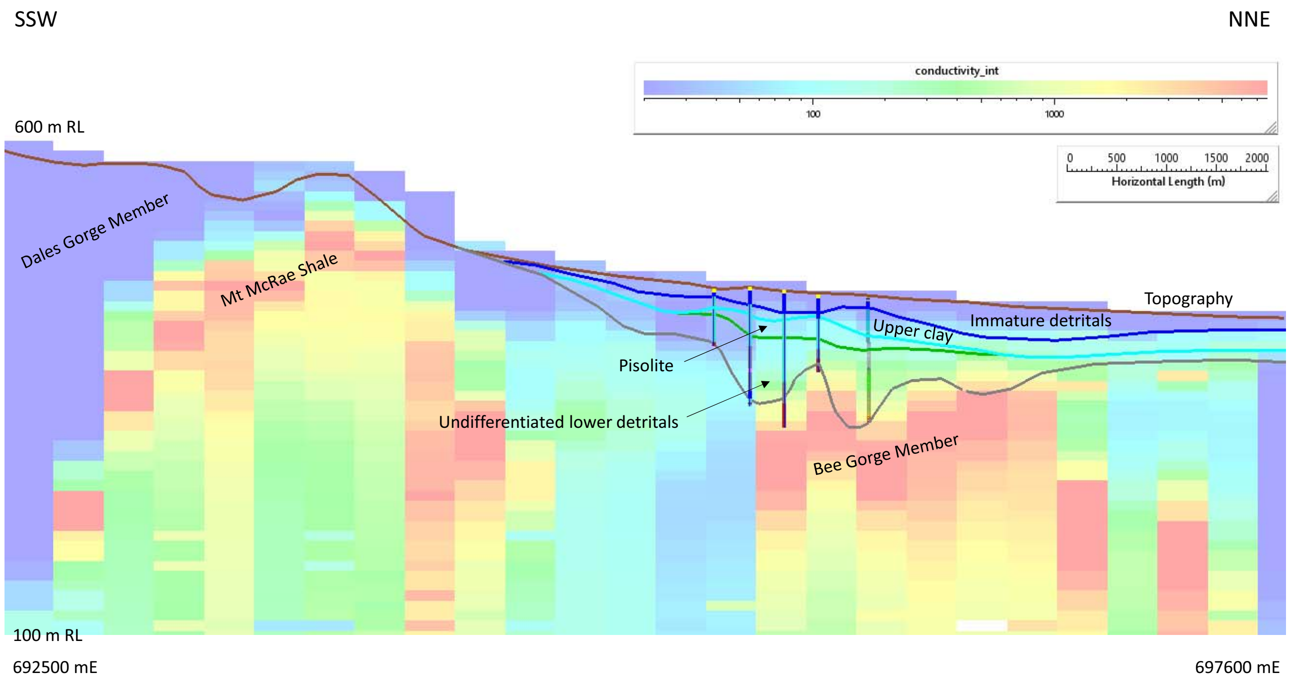

Figure 7 SSW-NNE section across the SkyTEM model, showing conductivity in mS/m. The total length of the section is ~11 km, and has a vertical exaggeration of 10:1.

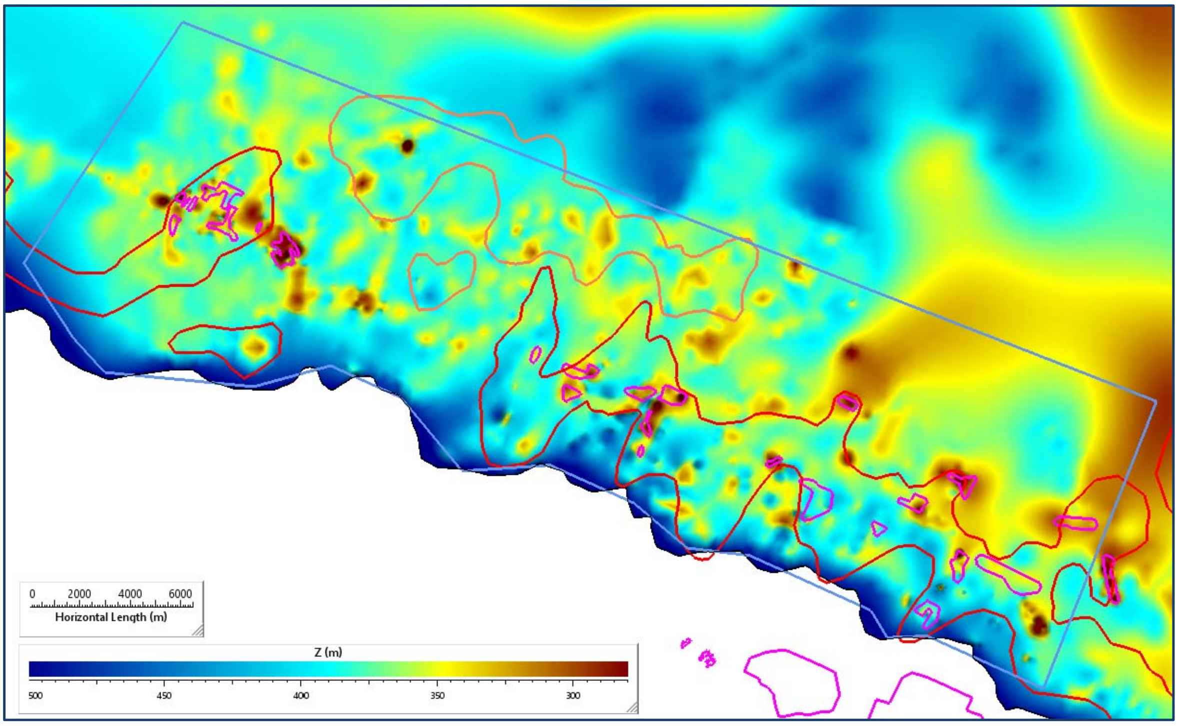

Figure 8 Basement model derived from SkyTEM AEM and drilling data, coloured by elevation. Known deposits are shown as pink polygons. Warmer colours denote basement depressions. The blue polygon shows the area of interest. Red and orange polygons denote the interpreted pisolites.

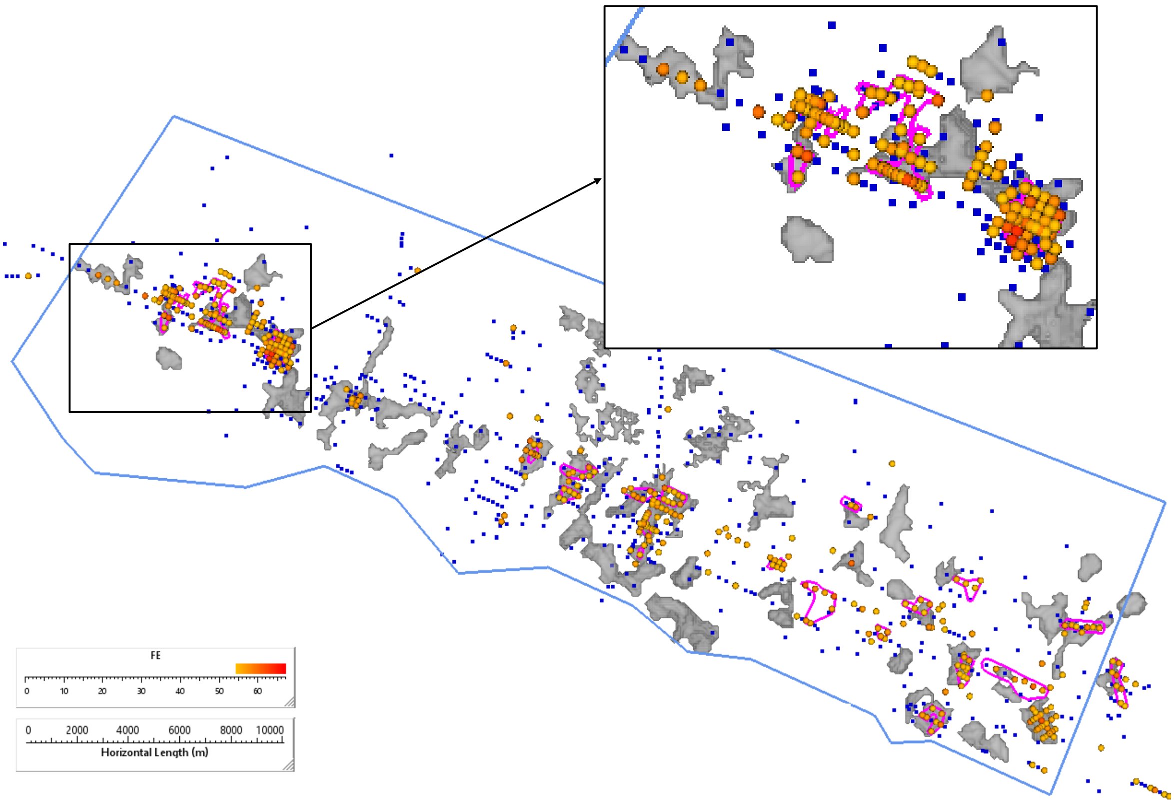

Figure 9 Excess mass from the SkyTEM AEM cover thickness model, showing drill holes and samples with >54% Fe.

CONCLUSIONS

Excess mass derived from ground gravity and interpreted cover thickness is spatially associated with known DID mineralisation. Nearly all known mineralisation is spatially associated with the pisolite unit, which can be identified from aeromagnetic data based on its characteristic mottled texture.

Two alternative approaches to calculation of excess mass from the ground gravity data have been attempted. The first of these used a cover thickness model derived from SRS and drilling data, and the second cover thickness interpreted from SkyTEM AEM data. Both cover models have some limitations. SRS generally matches the basement trend from drill hole logging but does not see to full depth in "sinkholes" where basement contact is deep, or in areas where high-velocity cemented units or calcretes occur within the detrital sequence. Interpretation of cover thickness from SkyTEM is complicated by the variable conductivity contrast between the cover and basement due to shale units within the basement, and by saline groundwater in the northeastern part of the area of interest. Robust interpretation of cover thickness from the SkyTEM data requires some drill hole control in order to help constrain the bedrock lithology.

Both approaches to calculation of excess mass have provided comparable results. In addition to identifying the known DID deposits, excess mass derived using both methods shows areas of potential mineralisation that have not been drill tested as well as possible extensions or alternate trends to known mineralisation.

REFERENCES

Christensen, N. B. and Tølbøll, R. J.,2009, A lateral model parameter correlation procedure for one-dimensional inverse modelling Geophysical Prospecting, **57**, 919-929.

Haederle, J. M., 2007, Koodaideri Central Detritals 3D Seismic Experiment and the potential role for Sparse Seismic Refraction to explore for Palaeochannel hosted Mineralisation: RTX Internal Memorandum, unpublished.

Krapež, B., Barley, M. E., and Pickard, A. L., 2003, Hydrothermal and resedimented origins of the precursor sediments to banded iron formation: sedimentological evidence from the Early Palaeoproterozoic Brockman Supersequence of Western Australia: Sedimentology, **50**, 979-1011.

Kneeshaw, M. and Morris, R.C., 2014, The Cenozoic detrital iron deposits of the Hamersley Province, Western Australia: Australian Journal of Earth Sciences, **61**, 513-586.